Indian Journal of Chemical Technology
Vol. 54, May 2025, pp. 407-417
DOI: 10.56042/ijct.v32i3.7278

Synthesis and application of corrosion inhibitor for hydrogen sulfide corrosion of steel

[1]Misirov Z. Kh., [2]Beknazarov Kh. S., [1]Akhmedov U.Ch., [1]Nomozov A.K. & [3]Babamuratov B. E.

[1]Department of Chemical Engineering, Termez State University of Engineering and Agrotechnologies, Termez, Uzbekiatan

[2]Department of General Medicine, Angren University, Angren, 110200, Uzbekistan

[3]Termiz University of Economics and Service, Termiz, 190111, Uzbekistan

*E-mail: abrornomozov055@gmail.com

Received 13 December 2023; accepted 6 February 2025

In this paper, the synthesis of PKA-1 brand oligomeric corrosion inhibitor based on polyethylene polyamine (PEPA) and crotonaldehyde has been done. In this synthesis, it is observed that the reaction efficiency is high when the molar ratio of the initial substances is 1:1 and the temperature is 50°C. The duration of the reaction is 2 h and dimethylformamide is used as a solvent. The structure of this synthesized compound has been studied by IR-spectrum methods. The inhibitory properties of the obtained PKA-1 brand corrosion inhibitor have been studied in the prevention of hydrogen sulfide corrosion of steel materials by gravimetric and electrochemical methods at different temperatures and time and at different concentrations of 50 mg/L, 75 mg/L, 100 mg/L and 150 mg/L. According to the obtained results, the inhibition efficiency increased as the inhibitor concentration increased, and the efficiency was 94.3% in OW (oil-water)+H_2S (400 mg/L) medium at a concentration of 150 mg/L. Also, the thermodynamic and kinetic parameters of the adsorption mechanisms of this corrosion inhibitor on the steel surface are studied, and the adsorption of this corrosion inhibitor on the steel surface is studied using Temkin, Frumkin and Langmuir isotherms. According to the results, it was found that the adsorption process proceeds according to the Langmuir isotherm. In addition, the surface morphology of steel is studied and analyzed with the help of scanning electron microscope and atomic force microscope.

Keywords: Corrosion inhibitor, Corrosion of steel, Hydrogen sulfide corrosion, PKA-1

Introduction

Despite the availability of corrosion inhibitors, there is an urgent need for effective inhibitors for the protection of metals against corrosion in various corrosive environments[1–3]. A corrosion inhibitor is a compound that is added in low concentrations to a corrosive solution to reduce and/or minimize the corrosion rate[4-6]. This effect is attributed to the adsorption of inhibitor particles on the metal surface resulting in the layer formation[7,8]. According to the results of international research conducted by NACE (IMPACT 2016), the annual economic damage of the corrosion process worldwide is 2.5 trillion US. It is concluded that, if we analyze this figure in each country section, it is about 3.4% of the average gross domestic product of each country[9]. The results of many years of scientific research carried out by world scientific community show that the environment should be taken into account when choosing corrosion inhibitors, and that the use of compounds containing nitrogen and sulfur and substances based on them is more effective for acidic environments. In addition, such as aldehydes, thioaldehydes, including various alkaloids, such as papaverine, strychnine, quinine, and nicotine, have been proven to be highly effective corrosion inhibitors and meet the requirements for corrosion inhibitors. Many researchers show that the use of corrosion inhibitors based on benzoates, nitrites, and inhibitors based on them, as well as chromates and phosphates, have a high inhibition efficiency for alkaline and acidic solutions[10,11].

In the oil and gas production industry, iron atoms in steel form Fe^{2+} ions, and these ions lead to forming derivatives of corrosion products with oxygen, hydrogen sulfide, or carbon dioxide. The extra electrons pass from the anode to the cathode, where water is reduced to form hydroxo ions. If there is no oxygen at the cathode, hydrogen ions turn into hydrogen gas. The anode and cathode regions are points where the electric potential differs. During the process, due to the formation of salts, electrolytes usually become electrolytes with higher electrical conductivity than water[12,13]. The main sources of corrosion in the oil and gas industry are hydrochloric

acid and its aqueous solutions, and they lead to hydrogen sulfide also carbon dioxide corrosion[14]. In the oil and gas industry, during the drilling and extraction processes, a corrosive environment is formed during treatment with acidic (HCl, HF, HNO_3, H_2SO_4, H_3PO_4, NH_2SO_2OH) and other solutions[15,16]. The most effective ways to prevent and control corrosion of structures based on different grades of steel are the development of coatings, cathodic protection, and corrosion inhibitors[17].

Experimental Section

Preparation of solutions and steel sample

The experiments were carried out with samples of carbon steel grade St20, having a chemical composition (wt.%): 0.24 C, 0.37 Si, 0.65 Mn, ~0.04 S, ~0.04 P, ~0.25 Ni , ~0.25 Cr, ~0.25 Cu, ~0.08 As, and ~98 Fe. Sodium sulfide and hydrochloric acid were used to create a hydrogen sulfide environment under laboratory conditions, and their concentration was measured by the iodometric titration method. The concentration of H_2S in the resulting working solution was (400 mg/L). Practical experiments were mainly carried out in hermetic devices with a capacity of 1000 mL.

Synthesis of PKA-1 oligomeric brand corrosion inhibitor

A chemical compound with the following formula was synthesized using polyethylene polyamine and crotonaldehyde (1:1) in the presence of dimethylformamide solvent when mixed at 50°C for 2 h as shown in Scheme 1. The obtained reaction mixture was cooled to room temperature and left for 24 h. The importance of the temperature and the mole ratio of the initial materials on the reaction yield was studied as shown in Table 1. This reaction has been carried out with the highest yield at a temperature of 50°C and a 1:1 mole ratio of the initial materials. The resulting product is a hard polymeric solid, soluble in alcohol and acetone, insoluble in water at normal temperature, but soluble at a slightly higher temperature.

Characterisation techinques

The functional groups of the synthesized PKA-1 corrosion inhibitor was studied using IR-spectrometer technology (IQ-Fure, SHIMADZU, Japan). A CS350 potentiostat-galvanostat was used to investigate the corrosion of steel St20. Weight loss measurements were carried out in a 1000 mL vessel without inhibitor and at different concentrations of PKA-1 inhibitor (50, 75, 100 and 150 mg/L) and at different times (24, 240 and 720 h). Oil water, OW+H_2S (400 mg/L) and OW+ CO_2 (105 Pa) media were selected as corrosive media. For electrochemical and gravimetric studies, steel plates measuring 1.0×3.5×0.1 cm were obtained from St20 steel. The oxide layer on the steel surface was removed by abrasive papers with from 400 to 1200 grades. The other organic contaminations and impurities were removed by acetone solvent.

SEM-YEVO MA 10 (Zeiss, Germany) was used to study the surface morphology of our metal samples. In this case, it is possible to obtain information such as the surface structure (external morphology), chemical composition, orientation of components, as

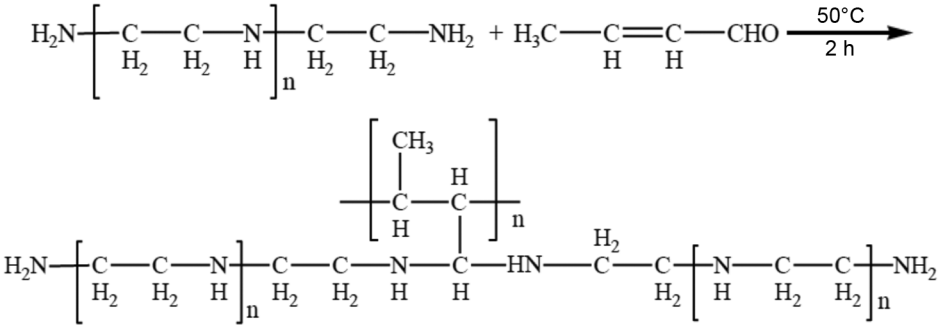

Scheme 1 — Synthesis of PKA-1 brand corrosion inhibitor

Table 1 — Effect of temperature on the formation of corrosion inhibitor PKA-1 based on PEPA and crotonaldehyde

Mole ratio of PEPA and crotonaldehyde	Temperature (°C)	Yield (%)	Temperature (°C)	Yield (%)
1:1	50	96.51	30	89.24
1:2		92.12		82.05
2:1		87.61		72.62

well as the crystal structure of the sample from the signals obtained from the electronic interaction of the analyzed sample. AFM-Agilent 5500 (Agilent, USA) was used with 145 with a hardness of 9.5 N/m^2 at a speed of up to 2.5-2.5-1 and 2.5-2.5-1 and 2.5-2.5-1 microns for studying the topography of the surface along the X-Y-Z axes of the St20 sample A silicon cantilever with kHz frequency was used[18]

Results and Discussion

Characterisation

IR spectroscopic analysis of corrosion inhibitor PKA-1

The IR spectrum of the synthesized PKA-1 (Fig. 1) displays absorption bands characteristic of its polyamide and vinyl-derived structure. The broad band at 3365 cm^{-1} corresponds to N–H stretching vibrations of primary and secondary amines. Peaks at 2935 cm^{-1} and 2860 cm^{-1} are assigned to aliphatic C–H stretching in –CH_2– and –CH_3 groups. A sharp, intense band at 1698 cm^{-1} is indicative of amide C=O stretching, confirming the formation of polyamide bonds via condensation with vinyl aldehyde. The 1555 cm^{-1} band is attributed to N–H bending (amide II) and/or C=C stretching of conjugated systems. Bands at 1452 cm^{-1} and 1384 cm^{-1} are due to CH_2 and CH_3 bending vibrations. The signal at 1265 cm^{-1} likely corresponds to C–N stretching of amide or amine groups. The 1152 cm^{-1} and 1027 cm^{-1} bands arise from C–O–C and C–N vibrations, respectively. The out-of-plane C–H deformation of substituted vinyl groups is observed at 892 cm^{-1} and 784 cm^{-1}, while the 657 cm^{-1} band is attributed to N–H wagging or skeletal deformation of amine functionalities.

Corrosion rate and inhibition efficiency

The inhibition efficiency and corrosion rate (K), also, weight loss (X) were determined based on the following formule:

$$K = \frac{(m_1 - m_2)\cdot 1000}{S\cdot \tau_1}\ [g/m^{-2}\cdot \text{day}] \quad \ldots (1)$$

$$X = \frac{K_{inh}}{K_0}\cdot 100,\ Z=100 - X,\ \% \quad \ldots (2)$$

Where, m_1 is the initial weight (g) of the sample, m_2 is the weight (g) of the metal sample after exposure, S is the surface area of the sample taken for the practical experiment, t_1 is the exposure time (h).

From the data presented in Table 2, for 24 h, the level of protection of corrosion inhibitor PKA-1 in OW + H_2S (400 mg/L) was found to be 81.3% at a concentration of 50 mg/L. From the data presented in Table 3, it follows that the level of protection of PKA-1 corrosion inhibitor in OW + H_2S (400 mg/L) was 82.3% at a concentration of 75 mg/L. Table 4 shows that the corrosion rate was high in aggressive environments where no corrosion inhibitor was used, and the protection level of PKA-1 corrosion inhibitor in OW + H_2S (400 mg/L) with a corrosion inhibitor was 85.3% at a concentration of 100 mg/L. From the data presented in Table 5, we can see that the

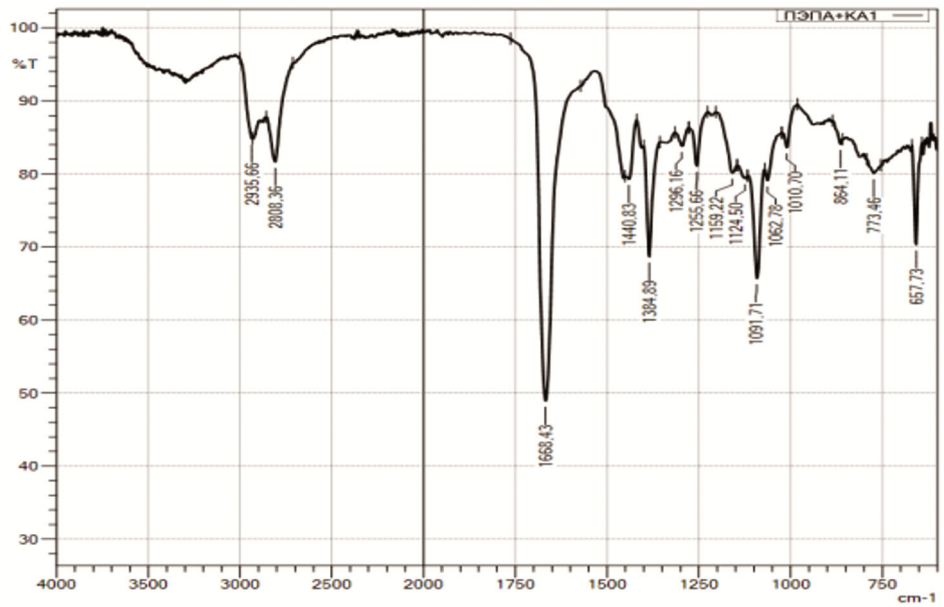

Fig. 1 — IR-spectrum of the corrosion inhibitor PKA-1

Table 2 — Protection level Z (%) on St20 steel using corrosion inhibitor of concentration 50 mg/L

t (h)	Indicators	Protection level Z (%)			
		Oil water (OW)	OW + H_2S (400 mg/L)	OW + CO_2 (105 Pa)	OW + H_2S (400 mg/l) + CO_2 (105 Pa)
24	K_0	0.413	0.721	0.351	0.586
	K	0.072	0.135	0.0635	0.116
	Z	82.6	81.3	81.9	80.2
240	K_0	0.169	0.245	0.112	0.256
	K	0.0285	0.045	0.0197	0.049
	Z	83.1	81.6	82.4	80.9
720	K_0	0.0565	0.0989	0.0576	0.134
	K	0.0104	0.019	0.0108	0.027
	Z	81.5	80.7	81.2	79.8

Table 3 — Protection level Z (%) on St20 steel using corrosion inhibitor of concentration 75 mg/L

t (h)	Indicators	Protection level Z (%)			
		Oil water (OW)	OW + H_2S (400 mg/l)	OW + CO_2 (105 Pa)	OW + H_2S (400 mg/l) + CO_2 (105 Pa)
24	K_0	0.431	0.728	0.387	0.612
	K	0.066	0.125	0.065	0.111
	Z	84.7	82.8	83.2	81.9
240	K_0	0.327	0.595	0.309	0.382
	K	0.048	0.098	0.049	0.067
	Z	85.3	83.5	84.1	82.5
720	K_0	0.208	0.305	0.223	0.297
	K	0.034	0.056	0.040	0.057
	Z	83.6	81.6	82.06	80.8

Table 4 — Protection level Z (%) on St20 steel using corrosion inhibitor of concentration 100 mg/L

t (h)	Indicators	Protection level Z (%)			
		Oil water (OW)	OW + H_2S (400 mg/L)	OW + CO_2 (105 Pa)	OW + H_2S (400 mg/L) + CO_2 (105 Pa)
24	K_0	0.453	0.711	0.392	0.598
	K	0.057	0.101	0.054	0.092
	Z	87.4	85.8	86.2	84.6
240	K_0	0.324	0.521	0.271	0.397
	K	0.0385	0.071	0.0346	0.058
	Z	88.1	86.3	87.2	85.3
720	K_0	0.211	0.351	0.151	0.267
	K	0.0286	0.052	0.0214	0.042
	Z	86.4	85.2	85.8	84.2

Table 5 — Protection level Z (%) on St20 steel using corrosion inhibitor of concentration 150 mg/L

t (h)	Indicators	Protection level Z (%)			
		Oil water (OW)	OW + H_2S (400 mg/L)	OW + CO_2 (105 Pa)	OW + H_2S (400 mg/L) + CO_2 (105 Pa)
24	K_0	0.413	0.671	0.381	0.613
	K	0.027	0.059	0.028	0.058
	Z	93.4	91.2	92.6	94.3
240	K_0	0.331	0.532	0.283	0.379
	K	0.0188	0.038	0.0195	0.0329
	Z	94.3	92.8	93.1	91.4
720	K_0	0.211	0.351	0.173	0.275
	K	0.015	0.033	0.015	0.031
	Z	92.8	90.6	91.5	88.6

corrosion rates were at high values in the aggressive environments where the corrosion inhibitor was not used, and then the corrosion rate slowed down and the level of inhibition increased in the environments where the corrosion inhibitor was used. The level of protection of corrosion inhibitor PKA-1 in OW + H_2S was 91.2% at a concentration of 150 mg/L.

Electrochemical measurements

Corrosion kinetic parameters such as E_{corr}, I_{corr}, β_a, β_c and percentage inhibition efficiency (%IE) obtained from the curves are recorded in Table 6 and 7. %IE is calculated by the following equation.

$$\%IE = (1 - I_{inh}/I_{uninh}) \times 100 \quad \ldots (3)$$

where I_{uninh} and I_{in} are corrosion current densities in non-inhibited and inhibited in the presence of PKA-1. It is clear that from the functions listed in Table 6, with increasing concentration of PKA-1, it can be seen that: the values of β_a and β_c are practically unchanged.

Potentiodynamic polarization analysis

potentiodynamic polarization (PDP) analyses were applied to test the inhibition behaviour of the studied steel working electrode in an aggressive medium and an inhibited environment (Figs 2 & 3). The corrosion current density (i^o_{PDP}) in the corrosive medium and (i^i_{PDP}) in the inhibited medium were calculated to calculate the inhibition efficiency ($\eta_{PDP}\ at\ \%$) (Eq. 4)[19]

$$\eta_{PDP}, \% = \frac{i^o_{PDP} - i^i_{PDP}}{i^o_{PDP}} \times 100\% \quad \ldots (4)$$

This indicates that PKA-1 is mixed-type inhibitor. This type of inhibitor works by adsorbing both anodic and cathodic sites on the surface of St20 carbon steel and thus delays the anodic dissolution of St20 and the cathodic H_2 evolution reaction. The E_{corr} values are not affected by the addition of PKA-1 inhibitor, the I_{corr} values decrease, which indicates the inhibitory effect of molecules. Thus, the %IE values increase by increasing the amount of PKA-1 inhibitor particles attached to the surface of St20 carbon steel[20,21].

Determination of activation thermodynamic parameters

Knowing the thermodynamic energy of the system is very important in determining the mechanisms of action of the corrosion inhibitor. Based on this, we can say that the energy of the thermodynamic system in which corrosion is occurring is measured in cases with and without an inhibitor taken at different concentrations. For this, it is found by applying the Arrhenius equation as follows.

$$CR = A\exp\left(\frac{-\mathrm{Ea}}{\mathrm{RT}}\right) \quad \ldots (5)$$

Where, E_a is the activation energy expressed in kJ/mol, R is the universal gas constant value of 8.314 J/mol K, T is the temperature expressed in K, is the pre-exponential coefficient[22].

If we compare the activation energy (E_a) of the solutions with an inhibitor to the solution without the inhibitor, we can see that E_a increases as a result of the addition of the inhibitor to the solution, and the activation energy also increases with the increase in the concentration of the inhibitor in the solution. A high activation energy causes physical adsorption, and if it does not change or becomes less, it causes chemical adsorption[23,24].

As the inhibitor concentration increased, the activation energy (E_a) values also increased dramatically.

Table 6 — Corrosion parameters determined according to the PDP of carbon steel St20 in uninhibited oil water solutions and taking into account various concentrations of PKA-1

PKA-1 concentration	Corrosion parameter				
	β_a (mV dec^{-1})	β_c (mV dec^{-1})	E_{corr} (mV) (SCE)	$I_{corr} \times 10^{-4}$ (mA cm^{-2})	IE (%)
Without inhibitor	115	139	-0.573	1.66	–
50 mg/L	113	140	-0.569	0.424	82.01
75 mg/L	112	141	-0.567	0.418	84.12
100 mg/L	116	143	-0.565	0.379	87.14
150 mg/L	117	145	-0.561	0.348	92.81

Table 7 — Corrosion parameters determined according to the PDP of carbon steel St20 in uninhibited oil water +H_2S(400 mg/L) solutions and taking into account various concentrations of PKA-1

PKA-1 concentration	Corrosion parameter				
	β_a (mV dec^{-1})	β_c (mV dec^{-1})	E_{corr} (mV) (SCE)	$I_{corr} \times 10^{-4}$ (mA cm^{-2})	IE (%)
Without inhibitor	114	136	-0.576	1.68	–
50 mg/L	112	138	-0.571	0.418	80.2
75 mg/L	111	140	-0.566	0.409	81.9
100 mg/L	115	141	-0.561	0.385	84.21
150 mg/L	116	144	-0.558	0.352	93.16

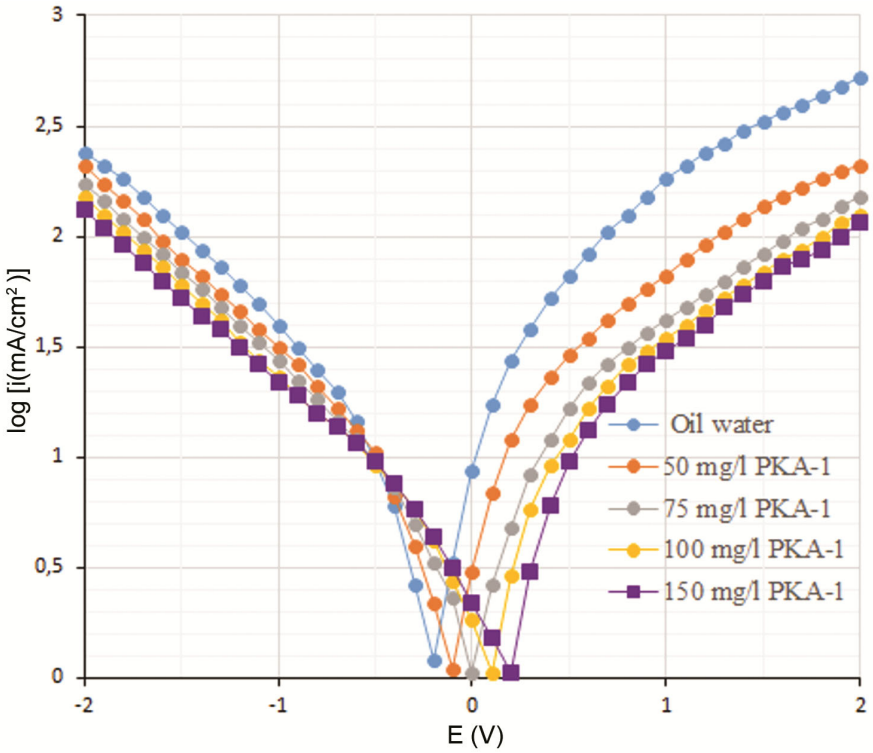

Fig. 2 — Potentiodynamic polarization plots of the steel samples after 24 h immersion in the oil water solutions without (Blank) and with different concentration of PKA-1

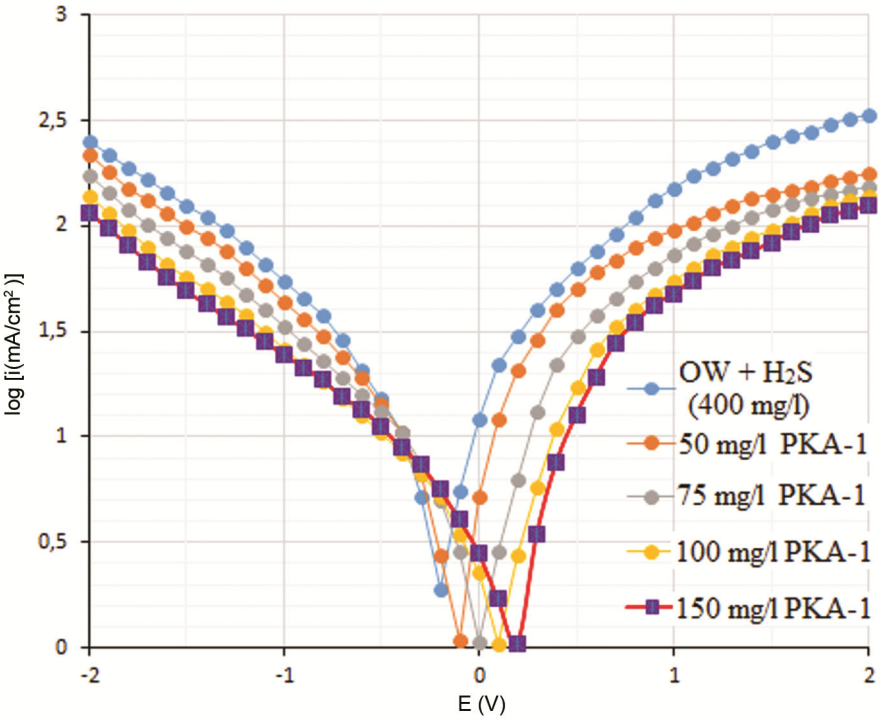

Fig. 3 — Potentiodynamic polarization plots of the carbon steel samples after 24 h immersion in the oil water+H_2S (400 mg/L) solutions without (Blank) and with different concentration of PKA-1

Therefore, in preventing corrosion, the primary function of the inhibitor is physical adsorption on the metal surface. From the large negative values of the entropies, we can see that the rate-determining step of corrosion, i.e., active complex formation, involves association rather than dissociation, which leads to a decrease in disorder[25,26]. In Fig. 4, Arrhenius plots were studied and used to determine activation energy values. The optimal concentration of PKA-1 corrosion inhibitor OW + H_2S (400 mg/L) in the environment was found to be 150 mg/L. The values of E_a obtained on the basis of Arrhenius graphs and data given in Table 8 show that two layers are formed on the surface of annealing St20 steel. Therefore, the value of Ea is high in solutions with added inhibitor, this value increases with the increase of inhibitor concentration, and the activation energy of the system also increases, increasing the inhibition efficiency.

Positive values of ΔH indicate that the melting process of St20 steel is endothermic. It should be noted that ΔH is 32.12 kJ/mol in the medium without inhibitor, with the addition of inhibitor to the solution, the value of ΔH increases with the increase of inhibitor concentration; for example, 46.81 kJ/mol at 50 mg/L, 69.40 kJ/moL at 75 mg/L, 91.66 kJ/mol at 100 mg/L, and 101.91 kJ/mol at 150 mg/L, of corrosion inhibitor PKA-1 which confirms that it maximally reduced the melting of St20 steel.

Also, in solutions without an inhibitor, the value of ΔS was -39.22 kJ/(mol·K), and with the introduction of an inhibitor into the system and its concentration increasing, its value was 84.18 J/mol (Table 8). As the concentration of PKA-1 corrosion inhibitor increases, the enthalpy value also decreases. In this case, a positive enthalpy value means that heat is absorbed.

Adsorption isotherm

The process of adsorption is desorption of water molecules by adsorbing inhibitor molecules on the metal surface, and this process can also be described as an exchange process. From this, we can see that the inhibitor is adsorbed on the metal surface and covers

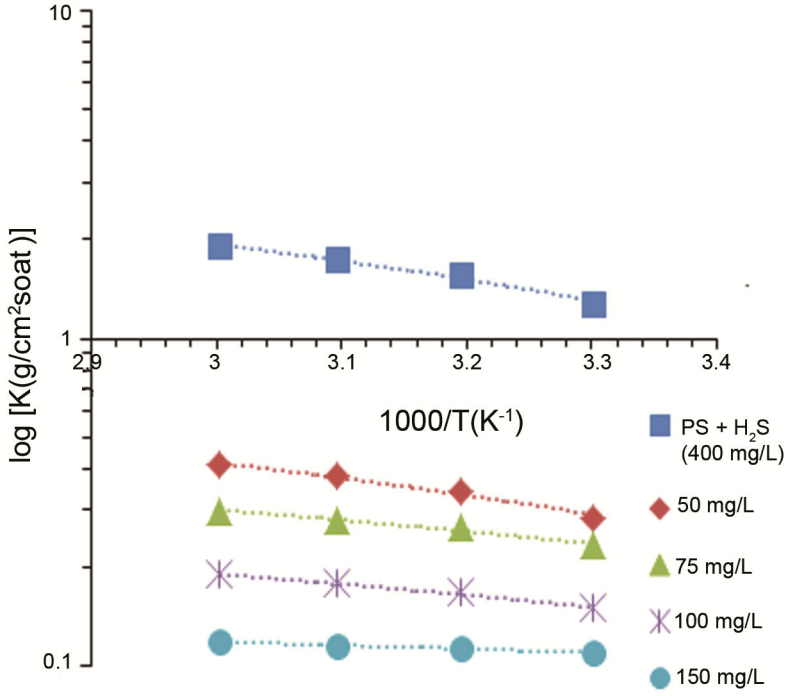

Fig. 4 — Arrhenius plot for activation energy of PKA-1 inhibitor in OW + H_2S (400 mg/L) solution

Table 8 — Kinetic and thermodynamic parameters of PKA-1 inhibitor in OW + H_2S (400 mg/L) solution

Parameter	Without inhibitor	PKA-1 concentration (mg/L)			
		50	75	100	150
E_a (kJ/mol)	40.30	48.14	70.12	92.53	105.56
ΔH (kJ/mol)	32.12	46.81	69.40	91.66	101.91
ΔS kJ/(mol·K)	-39.22	-19.35	48.22	61.20	84.18

the surface (θ) as the inhibitor concentration increases, the surface is covered to a higher degree and the efficiency increases. θ is a quantity indicating the effectiveness of the inhibitor and is taken as 100. To describe this process, the following adsorption isotherms of inhibitor were studied[27].

Langmuir: $\frac{C_{\text{ing}}}{\theta} = \frac{1}{K_{ads}} + C_{\text{ing}}$ … (6)

Frumkin: $\frac{\theta_{grav}}{1-\theta_{grav}} exp(-2f\theta_{grav}) = K_{ads}C_{ing}$ … (7)

Temkin: $exp(f\theta_{grav}) = K_{ads}C_{ing}$ … (8)

Where, C_{ing} is the concentration of the inhibitor in the solution (mg/L), θ-full coverage, K_{ads}-adsorption equilibrium constant.

The standard free energy of adsorption ($\Delta G°_{ads}$) is calculated by the following Eq. (8).

$$\Delta G^o_{ads} = \Delta H^o_{ads} - T\Delta S^o_{ads}$$

Where, R is the universal gas constant, T is the absolute temperature in Kelvin, and ρ_W is the density of water in g/L. The values of K_{ads} and $\Delta G°_{ads}$ are calculated using the above isotherm equations.

A negative value of $\Delta G°_{ads}$ indicates that the adsorption has reached a high peak. The value of $\Delta G°_{ads}$ showed a range of -40.5 kJ mol^{-1} and -43 kJ mol^{-1} for the Langmuir adsorption isotherm. The value of $\Delta G°_{ads}$ for the Temkin isotherm is between -32 kJ mol^{-1} and -40 kJ mol^{-1}. The value of $\Delta G°_{ads}$ - 40 kJ mol^{-1} is the equilibrium state of chemical and physical adsorption. If the value of $\Delta G°_{ads}$ is up to -20 kJ mol^{-1}, it is considered to represent physisorption, if the value of $\Delta G°_{ads}$ is more negative than -40 kJ mol^{-1}, it is considered to represent chemical sorption. Langmuir, Frumkin and Temkin isotherms of corrosion inhibitor PKA-1 in OW+H_2S (400 mg/L) medium were obtained[8] and plotted in Fig. S1 (Supplementary Information).

When studying the adsorption isotherms of corrosion inhibitor PKA-1, it can be concluded that the value of the correlation coefficients for the Frumkin (Fig. S1b) isotherm were 0.975, 0.9605, 0.9909 and 0.9899. The value of the correlation coefficients for the Temkin isotherm (Fig. S1c) were 0.9179, 0.9229, 0.9158 and 0.9213. It follows that the values of the correlation coefficients based on the Frumkin and Temkin isotherms are significantly different from 1, indicating that the PKA-1 brand corrosion inhibitor does not obey both of the above isotherms in the OW + H_2S (400 mg/L) environment. However, the value of the Langmuir isotherm showed values higher than 0.99, which shows us that the process is completely based on the Langmuir isotherm and is consistent with the data obtained on the basis of practical experiments in the calculation of thermodynamic parameters.

The Gibbs energy of the process was found using the values of the adsorption equilibrium constant (K_{ads}) at different temperatures using the Langmuir isotherm.

As shown in Table 9, the standard adsorption enthalpy ΔH^o_{ads} has a negative value (-13.15 kJ/mol), confirming that the adsorption of PKA-1 on carbon steel in OW + H_2S (400 mg/L) solution is an exothermic process. Furthermore, the negative value of the standard adsorption entropy ΔS^o_{ads}= -112.3 J/mol·K suggests that the adsorption film formed in this medium is highly stable. This stability arises from the inhibitor replacing the pre-adsorbed water molecules on the metal surface. From this, it can be concluded that this process fully corresponds and confirms the mechanism of inhibition.

SEM and AFM analysis

SEM and three dimensional AFM micrographs are provided from the surface of mild steel samples exposed to the OW+H_2S (400 mg/L) solutions without and with inhibitor to characterize the surface degradation[26]

Steel samples with dimensions of 3.2×2.4 ×1.8 cm were treated with sandpaper of different brands (No.400 - No.1200). Samples after treatment were placed in solutions with different concentrations of inhibitors and without inhibitors for 240 h. As can be seen from Fig. S2 (Supplementary information) the effectiveness of the corrosion inhibitor at a concentration of 150 mg/L is high[28,29].

The AFM micrographs and the corresponding roughness values for the mild steel specimens immersed in the OW + H_2S (400 mg/L) solutions

Table 9 — Thermodynamic parameters of adsorption of PKA-1 inhibitor in OW + H_2S (400 mg/L) solution obtained by Langmuir isotherm

Temperature (K)	K_{ads} (M^{-1})	ΔG^o_{ads} (kJ/mol)	ΔH^o_{ads} (kJ/mol)	ΔS^o_{ads} (J/mol K)
303	129.11	–19.2	-13.15	-112.3
313	142.31	–20.18		
323	167.8	–22.76		
333	219.17	–25.1		

without and with 150 mg/L PKA-1 are shown in Fig. S3. Results show that the roughness values in the presence of inhibitor are much lower than the one in the absence of inhibitor, reflecting the protective layer formation on the metal surface which inhibits the iron dissolution and surface damage.

In Fig. S3a, St20 steel surface is studied and analyzed at 4.5 x 4.5 mm, we can see that the size of the convex peaks in the solution without inhibitor is about 350 nm, while the size of the depressions is and it was 135 nm. It follows that the values of the concave and convex dimensions are high at this level, which means that the peaks are at a high level of corrosion. In Fig. S3b, in the inhibitor solution, the value of the convex peaks decreased from 350 nm to 100 nm, and the concave decreased from 135 nm to 60 nm. It is known that the surface of the annealed steel sample is significantly less convex than the surface of the non-annealed steel sample. It can be concluded that the inhibitors adsorbs on the surface and protects the surface against aggressive environments[30-34].

The research also evaluated different corrosion inhibitors based on their effectiveness in safeguarding carbon steel, highlighting their protection levels, molecular structures, and essential properties. The study examined the effectiveness of polyethyleneimine (PEI) as a corrosion inhibitor for ASTM 420 stainless steel in a 3% aqueous NaCl solution[35]. In another report HPAE-OHs, a third-generation hyperbranched polymer, as a green, cost-effective corrosion inhibitor is reported for Q235 steel in 1 M HCl. Synthesized via a simple solvent-free process, HPAE-OHs achieves 94.9% inhibition efficiency at 100 mg L^{-1} within 24 h, as confirmed by weight-loss tests[36]. The oxidation of water-oil mixtures due to CO_2, H_2S, or carboxylic acids accelerates steel corrosion. The efficiency of synthesized inhibitors based on oil and polyethylene polyamines with imidazolines were reported. At 80°C, in a mixture of 3% NaCl solution (200 cm^3), oil (800 cm^3), and acetic acid (0.5–3.0 g/dm^3), an inhibitor dose of 50 mg/dm^3 achieved 90–92% corrosion protection[37].

In contrast, PKA-1 exhibits a superior protection degree of 93.16%, making it the high effective among those compared. PKA-1 inhibitor is economic efficiency, combined with its environmentally friendly nature, distinguishing it from the primarily aromatic inhibitors. PKA-1's dual mechanism of physical and chemical adsorption, facilitated by multiple amine and imino groups, provides corrosion protection, making it a superior choice for protecting St20 steel in CO_2 and H_2S environments. PKA-1 is the cost-effectiveness and high protection efficiency, underscores its potential as an excellent corrosion inhibitor.

Conclusion

Inhibition properties of the compound synthesized on the basis of polyethylene polyamine and crotonaldehyde were studied in hydrogen sulfide environments. Its inhibition efficiency was studied by gravimetric and electrochemical methods. According to the results, its inhibition efficiency was 94.3%. The adsorption process of this PKA-1 brand corrosion inhibitor on the steel surface follows the Langmuir isotherm. In addition, the surface morphology studies indicated that for in steel surface coated with PKA-1 inhibitor, corrosion is very less compared to those without inhibitors.

Supplementary Information

Supplementary information is available on the website http://nopr.niscpr.res.in/handle/123456789.

References

1 Lagrenée M, Mernari B, Bouanis M, Traisnel M & Bentiss F, Study of the mechanism and inhibiting efficiency of 3,5-bis(4-methylthiophenyl)-4H-1,2,4-triazole on mild steel corrosion in acidic media, *Corros Sci*, 44 (2002) 573.

2 Gupta N K, Quraishi M A, Verma C & Mukherjee A K, Green Schiff's bases as corrosion inhibitors for mild steel in 1 M HCl solution: Experimental and theoretical approach, *RSC Adv*, 6 (2016) 102076.

3 Ostanov U Y, Beknazarov K S & Dzhalilov A T, Study by differential thermal analysis and thermogravimetric analysis of the heat stability of polyethylene stabilised with gossypol derivatives, *Int Polym Sci Technol*, 38 (2011) 25.

4 Wan K, Feng P, Hou B & Li Y, Enhanced corrosion inhibition properties of carboxymethyl hydroxypropyl chitosan for mild steel in 1.0 M HCl solution, *RSC Adv*, 6 (2016) 77515.

5 Zafar N, Khasan B & Abror N, Production of corrosion inhibitors based on crotonaldehyde and their inhibitory properties, *Int J Eng Trends Technol*, 70 (2022) 423.

6 Narzullaev A X, Beknazarov X S, Jalilov A T & Rajabova M F, Studying the efficiency of corrosion inhibitor IKTSF-1, IR-DEA, IR-DAR-20 in 1m HCl, *Int J Adv Sci Technol*, 28 (2019) 113.

7 Beknazarov K S & Dzhalilov A T, The synthesis of oligomeric derivatives of gossypol and the study of their antioxidative properties, *Int Polym Sci Technol*, 43 (2018) T25.

8 Avdeev Y G, Protection of metals in phosphoric acid solutions by corrosion inhibitors review, *Int J Corros Scale Inhib*, 8 (2019) 760.

9 Pedeferri M, Corrosion Science and Engineering, Milan, Italy: Springer, (2018) 9.

10 Rani B E A & Basu B B J, Green inhibitors for corrosion protection of metals and alloys: An overview, *Int J Corros*, 20 (2012) 380217.

11 Goncharova O A, Luchkin A Y, Andreev N N, Andreeva N P & Vesely S S, Triazole derivatives as chamber inhibitors of copper corrosion, *Int J Corros Scale Inhib*, 7 (2018) 657.

12 Kausalya T & Hazlina H, VGVG applied sciences review on corrosion inhibitors for oil and gas corrosion issues, *Appl Sci*, 10 (2020) 3389.

13 Nomozov A K, Beknazarov K, Khodjamkulov S, Misirov Z & Yuldashova S, Synthesis of corrosion inhibitors based on (Thio)Urea, Orthophosphoric acid and formaldehyde and their inhibition efficiency**,** *Baghdad Sci J*, 22 (2024) 458.

14 Szyprowski A, Methods of investigation on hydrogen sulfide corrosion of steel and its inhibitors, *Corros Corros Sci*, 59 (2003) 68.

15 Salman T A, Zinad D S, Jaber S H, Shayaa M, Mahal A, Takriff M S & Al-Amiery A A, Effect of 1,3,4 thiadiazole scafold on the corrosion inhibition of mild steel in acidic medium: An experimental and computational study, *J Bio-Tribo Corros*, 5 (2019) 1.

16 Beknazarov K S, Dzhalilov A T, Ostanov U Y & Erkaev A M, The inhibition of the corrosion of carbon steel by oligomeric corrosion inhibitors in different media, *Int Polym Sci Technol*, 42 (2015) T33.

17 Habeeb H J, Luaibi H M, Dakhil R M, Kadhum A A H & Gaaz T S, Development of new corrosion inhibitor tested on mild steel supported by electrochemical study, *Results Phys*, 8 (2018) 1260.

18 Durdibaeva R, Beknazarov K, Nomozov A, Demir M & Berdimurodov E, Exploring protective mechanisms with triazine ring and hydroxyethyl groups: Experimental and theoretical insights, *Kuwait J Sci*, 52 (2024) 100341.

19 Saraswat V & Yadav M, Improved corrosion resistant performance of mild steel under acid environment by novel carbon dots as green corrosion inhibitor, *Colloids Surf A*, 627 (2021) 127172.

20 Ghames A, Douadi T, Issaadi S, Sibous L, Alaoui K I, Taleb M & Chafaa S, Theoretical and experimental studies of adsorption characteristics of newly synthesized schiff bases and their evaluation as corrosion inhibitors for mild steel in 1 M HCl, *Int J Electrochem Sci*, 12 (2017) 4867.

21 Attabi S, Mokhtari M, Taibi Y, Abdel-Rahman I & Hafez B, Electrochemical and tribological behavior of surface-treated titanium alloy Ti–6Al–4V, *J Bio-Tribo Corros*, 5 (2019) 1.

22 Youssef A A A, Salas A H, Al-Harbi N, Basfer N M & Nassr D I, Determination of chemical kinetic parameters in Arrhenius equation of constant heating rate: Theoretical method, *Alex Eng J*, 67 (2023) 461.

23 Mohan R & Joseph A, Corrosion protection of mild steel in hydrochloric acid up to 313 K using propyl benzimidazole: Electroanalytical, adsorption and quantum chemical studies, *Egypt J Pet*, 27 (2018) 11.

24 Nomozov A K, Eshkaraev S C, Jumaeva Z E, Todjiev J N, Eshkoraev S S & Umirqulova F A, Experimental and theoretical studies of *Salsola oppositifolia* extract as a novel eco-friendly corrosion inhibitor for carbon steel in 3% NaCl, *Int J Eng Trends Technol*, 72 (2024) 312.

25 Shaymardanova M A, Mirzakulov K C, Melikulova G, Khodjamkulov S & Nomozov A, Studying of the process of obtaining monocalcium phosphate based on extraction phosphoric acid from phosphorites of central Kyzylkum, *Baghdad Sci J*, 22 (2024) 756.

26 Fouda A S, Abd-El-Maksoud A S, Zoromba M S & Ibrahim A R, Corrosion inhibition and thermodynamic activation parameters of Myrtus communis extract on mild steel in sulfamic and medium, *Int J Corros Scale Inhib*, 6 (2017) 428.

27 Selvi J A, Arthanareeswari A, Pushpamalini T, Rajendran S & Vignesh T, Effectiveness of Vinca rosea leaf extract as corrosion inhibitor for mild steel in 1N HCl medium investigated by adsorption and electrochemical studies, *Int J Corros Scale Inhib*, 9 (2020) 1429.

28 Qiang Y, Zhang S, Xiang Q, Tan B, Li W, Chen S & Guo L, Halogeno-substituted indazoles against copper corrosion in industrial pickling process: A combined electrochemical, morphological and theoretical approach, *RSC Adv*, 8 (2018) 38860.

29 Jawad Q A, Hameed A Q, Abood M K, Al-Amiery A A, Shaker L M, Kadhum A A H & Takriff M S, Synthesis and comparative study of novel triazole derived as corrosion inhibitor of mild steel in HCl medium complemented with DFT calculations, *Int J Corros Scale Inhib*, 9 (2020 688.

30 Akhmedov K N, Tadzhimukhamedov K S & Akhmedov U C, Synthesis of N, N-Diethylhydrazine and Its reactions with carboxylic acids and Alkyl Halides, *Russ J Gen Chem*, 75 (2005) 1720.

31 Turayev K K, Eshankulov K N, Umbarov I A, Kasimov S A, Nomozov A K & Nabiev D A, Studying of properties of bitumen modified based on secondary polymer wastes containing zinc, *Int J Eng Trends Technol*, 71 (2023) 248.

32 Akhmedov K N, Tadzhimukhamedov K S, Akhmedov U C, Tashkhodzhaev B B, Turgunov K K & Tozhiboev A, Reactions of N, N-diethylhydrazine with formic and o-benzoylbenzoic acids, *Russ J Gen Chem*, 77 (2007) 1337.

33 Yulchieva M G, Turaev K K, Nomozov A K & Tovoshareva I E, Studying synthesis of a chelate-forming sorbent based on urea-formaldehyde and diphenylcarbazone, *Indian J Chem*, 63 (2024) 579.

34 Nomozov A K, Beknazarov K S, Khodjamkulov S Z & Misirov Z K, Salsola Oppositifolia acid extract as a green corrosion inhibitor for carbon steel, *Indian J Chem Technol*, 6 (2023) 872.

35 Finšgar M, Fassbender S, Nicolini F & Milošev I, Polyethyleneimine as a corrosion inhibitor for ASTM 420 stainless steel in near-neutral saline media, *Corros Sci*, 51 (2009) 525.

36 Du S, Chen S, Zhang Z, Ye Z, Mao H, Yang H, Lian C & Bao C, Corrosion inhibition behavior of hydroxyl-terminated hyperbranched poly(amine-ester) for Q235 steel in HCl solution, *Mater Chem Phys*, 292 (2022) 126831.

37 Nikolai G, Inna T, Olena S, Oleksandr K & Olena H, Synthesis of high-effective steel corrosion inhibitors in water-oil mixtures, *East Eur J Enterp Technol*, 6 (2020) 6.